Iraqi Journal of Science, 2022, Vol. 63, No. 11, pp: 4705-4720
DOI: 10.24996/ijs.2022.63.11.10

ISSN: 0067-2904

Dielectric Breakdown Properties of He-H_2 Mixtures for High Temperature Superconducting Power Devices

Mohammad Mustafa Othman, Saeed Omer Ibrahim, Sherzad Aziz Taha*
Physics Department, College of Education, University of Salahaddin-Erbil, KRG, Iraq

Received: 20/8/2020 Accepted: 13/2/2022 Published: 30/11/2022

Abstract

In this study, the electron energy distribution function (EEDF), the electron swarm parameters , the effective ionization coefficients, and the critical field strength (dielectric strength) in binary He-H_2 gas mixture which is used as cryogenic for high-temperature superconducting power applications, are evaluated using two-term solution of the Boltzmann equation over the range of E/N (the electric field to gas density) from 1 to 100 Td (1 Td=10^{-17} Vcm^2) at temperature 77 K and pressure 2MPa, taking into account elastic (momentum transfer) and inelastic cross-sections. Using the electron energy distribution function (EEDF) electron swarm parameters (electron drift velocity, mean electron energy, diffusion coefficient, electron mobility, ionization and attachment coefficient) are calculated. At low reduced electric field strength E/N, the EEDF is close to Maxwellian distribution, at high E/N, due to vibrational excitation of H_2, the calculated distribution function is non-Maxwellian. Besides, the Boltzmann equation analysis showed as the small mole fraction of H_2 in the He-H_2 mixture is increased, the electron energy distribution function EEDF shifts to lower energy region, the density-reduced ionization coefficient α/N and density-reduced effective ionization coefficient (α-η)/N decreases, whereas density-reduced attachment coefficient η/N, density-reduced critical electric field strength increases, $(E/N)_{crt}$ and critical electric field E_{crt} increases. It is found that dielectric field strength depends on pressure and temperature. To confirm the validity of the two term solution of Boltzmann equation analysis, a set of elastic and inelastic cross-sections for each gas He and H_2 are used to calculate the electron swarm parameters and dielectric field strength. Compared with previous experimental and theoretical literatures, the values obtained are generally in good agreement.

Keywords: Boltzmann equation, electron swarm coefficients, cross-section sets, ionization and attachment coefficient.

خصائص العازل لمخاليط He–H_2 ذات درجة الحرارة العالية لأجهزة الطاقة فائقة التوصيل

محمد مصطفى عثمان، سعيد عمر ابراهيم، شيرزاد عزيز طه*
قسم الفيزياء، كلية التربية، جامعة صلاح الدين–أربيل، إقليم كردستان، العراق

*Email: sherzad.taha@su.edu.krd

الخلاصة

تم في هذه الدراسة، حساب دالة توزيع طاقة الإلكترون (EEDF) ، ومعاملات الحشد الإلكترون ، ومعاملات التأين الفعالة ، وقوة المجال الحرجة (قوة العزل) في خليط غاز الثنائي $He–H_2$ الذي يستخدم كمبردة لتطبيق طاقة فائقة التوصيل عالية الحرارة ، باستخدام تقريب ذي الحدين في معادلة بولتزمان لمدى E / N من 1 Td إلى 100 Td ($1\ Td = 10^{-17}\ Vcm^2$) عند درجة حرارة 77 K والضغط 2MPa ، مع الأخذ في الاعتبار المقاطع العرضية المرنة وغير المرنة.

استخدام دالة توزيع طاقة الإلكترون (EEDF)، لحساب معاملات الحشد الإلكترون (سرعة انجراف الإلكترون، متوسط طاقة الإلكترون، معامل الانتشار، قابلية انتقال الإلكترون، معامل التأين ومعامل ارتباط). عند شدة المجال الكهربائي E / N المنخفض، يكون توزيع طاقة الإلكترون قريبًا من توزيع Maxwellian، وعند مجالات E / N العالية، نظرًا للإثارة الاهتزازية لجزيئة H_2، تكون دالة التوزيع المحسوبة غير Maxwellian. إلى جانب ذلك، أظهر تحليل معادلة بولتزمان مع زيادة نسبة قليلة من H_2 في خليط $He–H_2$ ، وجد أن دالة توزيع طاقة الإلكترون تتحول إلى منطقة طاقة أقل ، ومعامل α / N ايضا معامل التأين الفعال $(\alpha–\eta) / N$ ، في حين أن معامل التعلق η / N ، و شدة المجال الكهربائي الحرج $(E / N)_{crt}$ والمجال الكهربائي الحرج E_{crt} يزداد. لقد وجد أن شدة المجال العازل تعتمد على الضغط ودرجة الحرارة. لتأكيد صحة حل تقريب ذي الحدين في معادلة بولتزمان، تم استخدام مجموعة من المقاطع العرضية المرنة وغير المرنة لكل غاز He و H_2 لحساب معلمات سرب الإلكترون وشدة المجال العازل ومقارنة بالنتائج التجريبية و النظرية السابقة.

1. Introduction

Hydrogen gas is the lightest diatomic gas, colourless, odourless, non-metallic, tasteless, highly flammable, and non-toxic but is asphyxiated by separation (up losing) oxygen in the air. Hydrogen gas is used in several industrial applications, i.e. maritime, domestic energy, electricity generation, and superconductor applications. A superconductor is a material with zero resistance which was discovered by Kamerlingh in 1911. They are classified into two groups according to their critical temperature: Low Temperature Superconductor (LTS) whose critical temperature is below 30K, and High Temperature Superconductor (HTS) whose critical temperature is above 30K. High temperature superconductors (HTS) are used for power applications useful in aerospace and naval applications [1].

Gaseous helium (GHe) is the preferred cryogen for high temperature superconducting (HTS) applications that work at temperatures lower than 77 K to produce a higher critical current density. However, gaseous helium GHe is chosen as cooling media for certain high temperature superconducting HTS power applications, in which reduced asphyxiation hazard and wider operation temperature range [2]. It is preferable to use GHe as a cryogen because of its low dielectric strength compared to that of liquid nitrogen LN2, which limits the applicability of GHe to low voltage power devices. At cryogenic temperatures the dielectric strength of GHe is lower than that of hydrogen gas. Graber et al. showed that a small mole fraction of H_2 in He-H_2 mixture increased the ac breakdown voltage compared to pure GHe [3].

In Cryogenic He-H_2 mixtures, the Electron Energy Distribution Function(EEDF) is the most important parameter to calculate the dielectric strength of gases and electron swarm parameters, i.e. electron mobility (μ_e), diffusion coefficient (D), mean electron energy (ε), characteristic energy (D/μ_e), drift velocity (v_d), ionization (α) and attachment (η) coefficient as well as the critical reduced electric field strength $(E/N)_{crt}$ at which the density-reduced ionization coefficient (α/N) and reduced attachment coefficient (η/N) are in balance ($\alpha/N= \eta/N$). All these parameters are calculated by the electric field strength E/N, using the two-term

solution of Boltzmann equation analysis. E/N is expressed in units of Townsend (Td), where ($1Td=10^{-17}$ $V.cm^2$).

Several workers used non-cryogenic temperature to calculate the electron swarm parameters and dielectric field strength using Boltzmann equation analysis under an applied dc electric field. For example, Pinheiro and Loureiro [4] studied the effective ionization coefficient (α-η)/N of hexafluoride SF_6 and its mixtures with helium He and xenon Xe, respectively. Zhao et al. [5] investigated the critical reduced electric field strength for CO_2 and its mixtures with 50% O_2 and 50% H_2 from Boltzmann equation analysis at various gas temperature and atmospheric pressure. Tezcan et al. [6] used the two-term solution of Boltzmann equation analysis to study the electron swarm parameters and dielectric field strength in binary CF_4–Ar mixtures by varying the mole fraction of CF_4 which is considered as a potential SF_6 replacement gas. Deng et al. [7] used C_3F_8 as an insulation medium because it has strong electronegative property to study the critical breakdown electric field of C_3F_8-CO_2 and C_3F_8-N_2 gas mixtures, while carbon dioxide CO_2 and nitrogen N_2 gas were used in order to increase the vapour pressure of the mixtures.

Many workers have used density reduced critical electric field $(E/N)_{crt}$ as a metric to calculate the dielectric strength of gas mixtures at 10-100 K cryogenic temperature and pressure used in HTS over the range 1.0 and 2.0 MPa. Hence, it is necessary to select the allowed mole fraction of gas mixtures to examine greater $(E/N)_{crt}$ over the cryogenic temperature range. The best choice of gases for cryogenic applications are H_2, He, N_2, O_2, and F_2: their Paschen's curves of their pure form are widely available [24]. One of the challenges posed by gaseous helium GHe is its non-electronegativity and low dielectric medium. Dielectric strength of He-based gas mixtures with varying mole fraction of H_2, Ne and N_2 (binary mixture) over a wide range of temperature and pressure under cryogenic temperature have been reported by several literatures [8,9].

Recently Park et al. used Paschen's model to estimate dielectric strength of binary He-H_2 and ternary He-H_2-N_2 cryogenic gas mixtures [10].

In this research, the electron swarm parameters and the density reduced ionization and attachment coefficient of H_2 gas and He-H_2 gas mixtures were calculated using two term solution of Boltzmann equation analysis at a critical temperature of 77 K over the range $1 \leq E/N \leq 100$ Td, where ($1Td=10^{-17}$ $V.cm^2$). From the Electron Energy Distribution Function (EEDF) the density-reduced critical electric field strength $(E/N)_{cr}$ was calculated by balancing electron generation α/N and electron loss η/N, where N is the total number density.

2. Boltzmann Equation Analysis

The electron energy distribution function (EEDF) is an important physical parameter used to calculate the reaction rate for the electron collision reactions and electron swarm parameters using two-term solution of Boltzmann equation. The relationship between the electron swarm parameters and collision cross sections of electron with the neutral particles (elastic and inelastic) through the electron energy distribution function is illustrated in the chart:

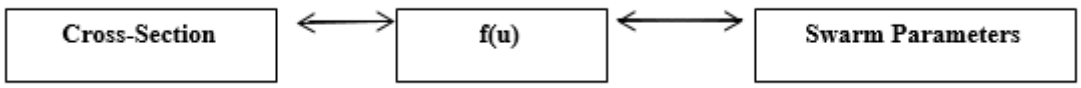

Consider an electron gas drifting (V/cm) in uniform dc applied electric field E with a velocity distribution *f*(*v*), the general form of the Boltzmann equation that describes the evolution of the distribution function in six-dimensional space is [11]:

$$\frac{\partial f(v)}{\partial t}+v\nabla_r f(v)-\frac{eE}{m}.\nabla_v f(v)=\left(\frac{\partial f}{\partial t}\right)_{oll} \quad (1)$$

$$\left(\frac{\partial f}{\partial t}\right)_{coll}=\left(\frac{\partial f}{\partial t}\right)_{el}+\left(\frac{\partial f}{\partial t}\right)_{in} \quad (2)$$

Where: ∇_r is the space gradient operator in three dimensions, ∇_v is the velocity gradient operator in three dimensions, v is the velocity and $\left(\frac{\partial f}{\partial t}\right)_{coll}$ is the collision operator due to elastic and inelastic collisions of electron with the neutral particles such as excitation, ionization and attachment. When space gradient is negligible $f(r,\bar{v},t)=f\left(\bar{v},t\right)$ and $\nabla_r f=0$, the equation for one kind of particle can be written as:

$$\frac{\partial f(v)}{\partial t}-\frac{eE}{m}.\nabla_v f(v)=\left(\frac{\partial f}{\partial t}\right)_{coll} \quad (3)$$

To solve Equation (3), the distribution function *f(v)* is expanded in term of spherical Legendre functions:

$$f(\bar{v})=\sum_{\lambda=0}^{\infty} f_\lambda(v)P_\lambda(\cos\theta) \quad (4)$$

Only the first two terms approximation of the distribution function *f(v)* are considered, when the mean random velocity is greater than the drift velocity.

$$f(\bar{v})=f_o(v)+\frac{\bar{v}}{v}f_1(v) \quad (5)$$

Where: $f_o(v)<<f_1(v)$, $f_o(v)$ and $f_1(v)$, the isotropic and anisotropic parts, respectively are a function of *v* (the magnitude of $\bar{v}$ only), which are obtained by substituting Equation (5) into Equation (3), resulting in two coupled equations [11]:

$$\frac{-\partial f_1}{\partial t}+\frac{eE}{m}\frac{\partial f_o}{\partial v}=\frac{f_1}{\tau} \quad (6)$$

$$\frac{\partial f_o}{\partial t}-\frac{1}{mv^2}\frac{\partial}{\partial v}\left(\frac{ev^2}{3}E.f_1+\frac{m^2}{M}NQ_m v^4 f_o+\frac{mK_BT}{M}NQ_m v^3\frac{\partial f_o}{\partial v}\right)=\left(\frac{\partial f_o}{\partial t}\right)_{in} \quad (7)$$

In Equation (7), the right term $\left(\frac{\partial f_o}{\partial t}\right)_{in}$ indicates inelastic collisions only, τ is the relaxation time in picoseconds. Assume all quantities in Equation (6) to be time independent, the solution is:

$$f_1=\frac{eE\left(\frac{\partial f_o}{\partial v}\right)}{mNvQ_m}+\exp\left(-\frac{t}{\tau}\right) \quad (8)$$

$$\tau=\left(NvQ_m\right)^{-1} \quad (9)$$

during this time scale, the value E or N does not change, then f_1 is given by:

$$f_1 = \frac{eE\left(\frac{\partial f_o}{\partial v}\right)}{mN\nu Q_m} \tag{10}$$

Making a change in the independent variable $u=mv^2/2e$, the steady state electron energy distribution function *f(u)* obtained by solution of the Boltzmann equation may be written in the form [12]:

$$\begin{aligned}
&\frac{E^2}{3}\frac{d}{du}\left(\frac{u}{NQ_m(u)}\frac{df_0(u)}{du}\right)+\frac{2m}{M}\frac{d}{du}\left(u^2NQ_m(u)f_0(u)\right)\\
&+\frac{2mK_BT_g}{Me}\left(u^2NQ_m(u)\frac{df_0(u)}{du}\right)\\
&+\sum_J\left[(u+u_J)f_o(u+u_J)N_oQ_J(u+u_J)-uf_o(u)N_oQ_J(u)\right]\\
&+\sum_J\left[(u-u_J)f_o(u-u_j)N_JQ_{-J}(u-u_J)-uf_o(u)NQ_{-J}(u)\right]=0
\end{aligned} \tag{11}$$

Here, e, m, M, K_B, and u are the electron charge, electron mass, molecular mass, Boltzmann constant and electron energy, respectively, and N is the number density of molecules per cm^3. $Q_m(u)$ is the momentum transfer cross-sections related to the total cross section $Q_m(u)= Q_T(u)(1-\cos\theta)$, where θ is the scattering angle. $Q_J(u)$, and u_J are excitation (rotational, vibrational, electronic) cross- section and energy loss due to collisional excitation, respectively. The last two terms are the influence of superelastic collisions occurring at low electric field, $Q_{-J}(u)$ is superelastic cross-section, u_J energy gain due to superelastic collision. The superelastic cross-section Q_{-J} can be written as [11]:

$$Q_{-J} = \frac{u+u_J}{u}Q_J(u+u_J) \tag{12}$$

EEDF, obtained by Equation (11), is an important physical parameter for calculating the electron swarm parameters and reaction rates. At low electron energy and thermal equilibrium, the elastic collision dominates, while inelastic collision (excitation and ionization) requires higher electron energy to occur, which play the main role in the dropping of EEDF or shifting it left or right to coincide with the decrease or increase of mean electron energy and kind of gas mixtures.

In the case of thermal equilibrium, the EEDF chosen as a Maxwellian function with temperature T_e is given by:

$$f(u) = \frac{2}{\sqrt{\pi}}.\sqrt{\frac{1}{(K_BT_e)^3}}.\sqrt{u}.\exp\left(\frac{u}{K_BT_e}\right) \tag{13}$$

With a mean electron energy of :

$$\bar{u} = \frac{3}{2}K_BT_e \tag{14}$$

where K_B is Boltzmann constant, equal to one when electron temperature expressed in unit of energy (in eV). The EEDF normalized by:

$$\int_0^\infty \sqrt{u}\,f_o(u)du = 1 \tag{15}$$

The electron swarm parameters are expressed in terms of electron energy distribution function EEDF ($f_o(u)$ in $eV^{-3/2}$) and total effective momentum transfer cross-section as follows [13]:

The mean electron energy (eV):

$$\bar{u} = \int_0^\infty u^{\frac{3}{2}} f_o(u) du \tag{16}$$

The electron mobility μ_e ($cm^2/V.s$):

$$\mu_e = -\frac{1}{3N}\left(\frac{2e}{m}\right)^{1/2} \int_0^\infty \frac{u}{Q_T(u)} \frac{df_o(u)}{du} du \tag{17}$$

The electrons drift velocity v_d (cm/s):

$$v_d = \mu_e E \tag{18}$$

The transverse diffusion coefficient D_T (cm^2/s):

$$D_T = \frac{1}{3N}\left(\frac{2e}{m}\right)^{1/2} \int_0^\infty \frac{u f_o(u)}{Q_T(u)} du \tag{19}$$

Here, $Q_T(u)$ is total effective momentum transfer cross-section, given by:

$$Q_T(u) = Q_{ela.}(u) + \sum Q_{inel.}(u) \tag{20}$$

Where: $Q_{ela.}(u)$ is the elastic (momentum transfer) cross section. The term $\sum Q_{inel.}(u)$ includes all the excitation cross-sections of discrete (rotational, vibrational, electronic) states. The reduced-density ionization coefficient α/N (cm^2) is given by [14]:

$$\frac{\alpha}{N} = \frac{1}{v_d}\left(\frac{2e}{m}\right)^{1/2} \int_i^\infty Q_i(u) u f_o(u) du \tag{21}$$

Where $Q_i(u)$ is the ionization cross-section.

The reduced-density attachment coefficient η/N (cm^2) is given by:

$$\frac{\eta}{N} = \frac{1}{v_d}\left(\frac{2e}{m}\right)^{1/2} \int_a^\infty Q_a(u) u f_o(u) du \tag{22}$$

Where $Q_a(u)$ is the attachment cross-section.

The reduced critical electric field strength $(E/N)_{crt}$ is obtained when the creation and loss electrons reach a balance:

$$\frac{\alpha}{N} = \frac{\eta}{N} \tag{23}$$

In this case the effective ionization coefficient $\alpha_{eff.}=(\alpha-\eta)/N$ is equal to zero [15].

The values of electron energy distribution function as a function of electron energy *f(u)* are obtained from Boltzmann's equation using all the electron collisional cross-sections.

3. Cross Section

The data of electron collision cross-sections which is the interaction between electrons and neutral gases is the most fundamental factor, used as the input data to calculate electron swarm parameters in He-H_2 gas mixtures. The elastic and inelastic cross-sections used in the present analysis for H_2 molecule and He atom are explained below which were taken from Kieffer [16]. The set cross-sections for H_2 molecule includes one momentum transfer cross-section, three vibrational excitation cross-sections (v_1, v_2, v_3) with threshold energy of 0.027, 1.03 and 1.864 eV, respectively, two electronic excitation cross-sections with threshold

energy of 8.85 eV and 12.0 eV, one dissociative attachment cross section with threshold energy of 3.56 eV, and one ionization cross section with 15.427 eV threshold energy.

The set of collisional cross-sections for He atom includes one momentum transfer cross-section, three electronic excitation cross-sections ($^{1}_{2}P$, $^{3}_{2}P$) with threshold energy of 21.203 eV and 20.949 eV, respectively, ($^{1}_{3}P$) with threshold energy of 23.071 eV, and one ionization cross-section with threshold energy of 24.586 eV. In the present work, the electron energy distribution function was calculated from the two- term solution of Boltzmann equation analysis for the energy using NOMAD code [17]. Therefore, all the electron kinetics including elastic and inelastic cross-sections of H_2 and He should be taken into consideration to calculate the electron swarm parameters namely, electron drift velocity, diffusion coefficient, electron mobility, mean electron energy, ionization coefficient, attachment coefficient and reduced critical electric field strength in He-H_2 gas mixture.

4. Results and discussion

Hydrogen is an active and the main attaching gas in the He-H_2 gas mixture; it differs from helium gas that it has vibrational levels and dissociation attachment. The electron collision cross-sections of He and H_2, explained in the previous section, were used as the main input data to calculate the electron swarm parameters to solve the electron energy distribution function (EEDF) based on the two-term solution of Boltzmann equation.

This calculation was focused on the density reduced ionization and attachment coefficient, where the density reduced critical electric field strength $(E/N)_{crt}$ in He-H_2 mixtures was in the range from 1 to 100 Td at critical temperature 77 K and pressure 2 MPa. The mixing ratio of the H_2 in the mixtures was from 20% H_2 to 1% H_2.

The electron energy distribution function (EEDF) as a function of electron energy were obtained using the two-term solution of Boltzmann equation method, Equation (11), at different values of electric field strength E/N.

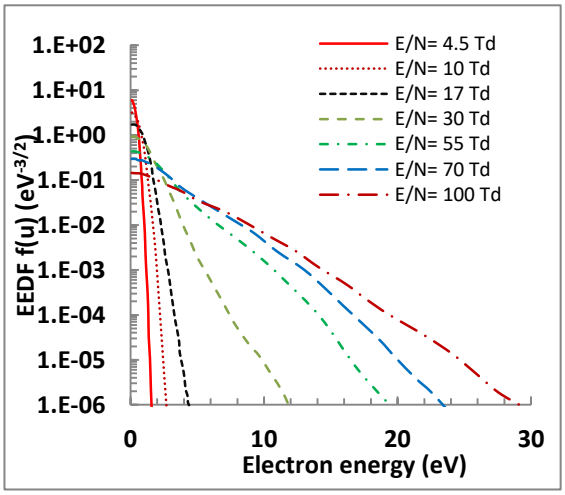

Figure 1: Electron energy distribution function as a function of electron energy for pure H_2 at T=77K.

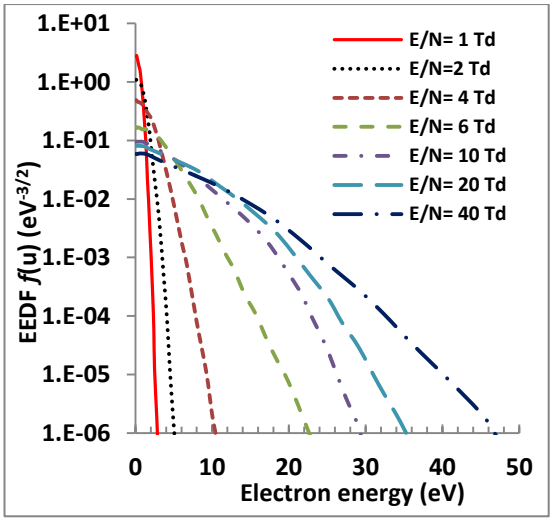

Figure 2: Electron energy distribution function as a function of electron energy for pure He at T=77K

The calculated EEDF for a dc applied field in H_2 and He at different values of E/N at a temperature of 77K and 2MPa pressure are shown in Figures 1 and 2, respectively. It was found that at the lowest electric field strength E/N, the electron energies were thermal and the electron energy distribution function (EEDF) was Maxwellian Equation (13) with mean electron energy $\bar{u} = 1.5K_B T_e$, where T_e is in unit of eV. The Maxwellian distribution function normalized by Equation (15) decreased sharply after several (eV). When E/N<17 Td for pure H_2 and E/N≤2 Td for pure He, the Maxwellian function were straight lines, because the elastic and inelastic cross-sections are constant at low electric field, in this region the degree of ionization is very small. However, for higher E/N values, the EEDF in H_2 and He were clearly non-Maxwellian, and had a shoulder at about 3 eV when E/N≥10 Td, due to the large electronic excitation and vibrational cross-section; in case of H_2 the vibrational cross-section is equal to $5.1\text{x}10^{-16}$ cm^2 at 3 eV. As shown in Figures 1 and 2, the tail of the distribution function shifted to higher energy due to inelastic collisions which reflect the dominant electron molecule energy exchange processes; in this region more ionization or excitation collisions occur, then the mean electron energy increases with increasing E/N, as shown in Figure 3. EEDF as function of electron energy for a fixed value of E/N=10 Td at temperature 77 K and pressure 2 MPa, are shown in Figure 4, for pure He, pure H_2, and for different concentrations of He and H_2 in the He-H_2 gas mixture. The pure H_2 has high EEDF at low electron energy compared to that of He. EEDF has changed by adding small mole fractions of H_2 in the He-H_2 gas mixture. For electron energy ≤3 eV, the EEDF increased with increasing H_2 mole fraction in the mixture. However, at electron energy > 3 eV the EEDF decreased.

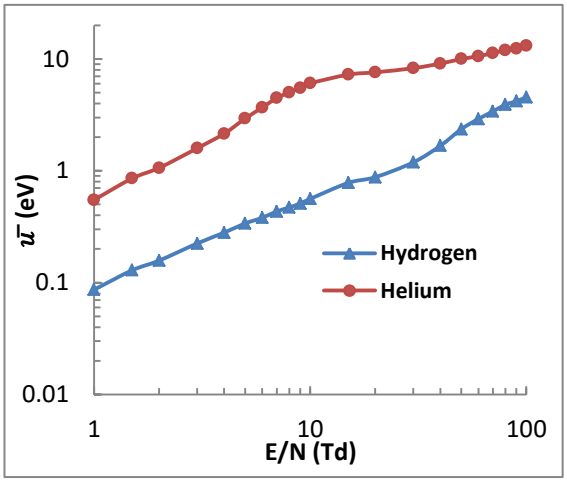

Figure 3: Mean electron energy as a function of electron energy.

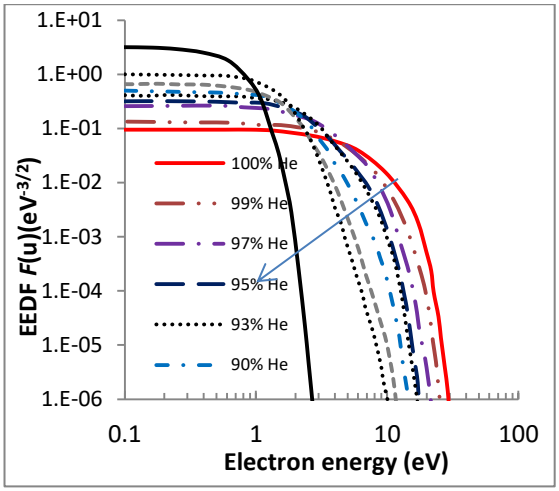

Figure 4: Electron energy distribution function for He-H_2 mixtures at E/N=10 Td

The tail shifted to the left, this is because the threshold energy at the vibration level (v_1) of H_2 gas is 0.027 eV. For this reason, the inelastic collision of electrons with H_2 molecules occurred at low E/N values, there are only little number of electrons that have energies greater than the ionization potential. As the ratios of H_2 in the mixture were increased, the degree of ionization and the number of particles with energies higher than excitation energy decreased which tend to increase the attachment process.

To emphasize the validity of two-term solution of Boltzmann equation analysis, the electron drift velocity, and reduced density ionization coefficient values of the present study were compared with previous experimental and theoretical literatures. The values of drift velocity of H_2 at temperature 77 K as a function of E/N are shown in Figure 5. The present

results were compared with the experimental values of Roznerski and Leja [19] and theoretical values of Engelhardt and Phelps [18], Thi Lan and Jeon [20], and Raju [21]. The present results agree well over the common E/N range. The present values of drift velocity for He, shown in Figure 6, are in good agreement with the previous experimental values of Kucukarpaci[22] and theoretical values of Raju [21] and Tuan [23].

The density-reduced ionization coefficient α/N were calculated at temperature 77 K and pressure 2 MPa, using the two-term solution of Boltzmann equation. In the case of H_2, the results were obtained over the range 45≤E/N≤100 Td. Figure 7 shows α/N as a function of E/N, compared with the experimental values of Rose [25], and Shallal and Harrison [26] and theoretical values of Engelhardt and Phelps [18], Raju [21], and Lieberman and Lichtenberg [24], good agreement was observed. Figure 8 shows α/N in He over the range 10≤E/N≤100 Td, also plotted for comparison were the measured values of Chanin and Rork [27], Lakshminarasimha et al.[28] and theoretical values of Raju [21], Lieberman and Lichtenberg [24], showing good agreement. However, at high E/N≥145 Td the experimental values of Lakshminarasimha et al.[28]were lower than the present results. The coherent results obtained confirmed that the two-term solution of Boltzmann equation analysis of the present study is valid.

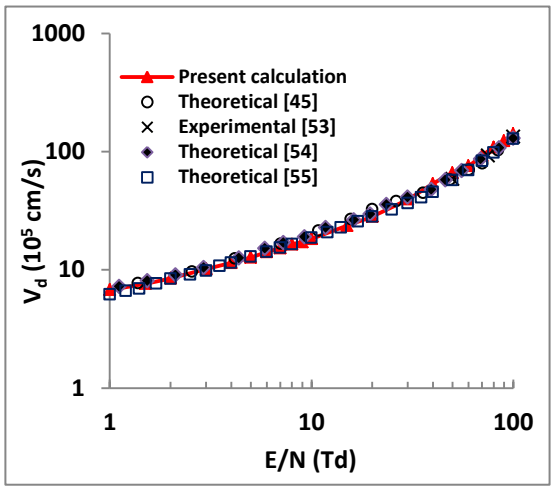

Figure 5: Electron drift velocity in pure hydrogen.

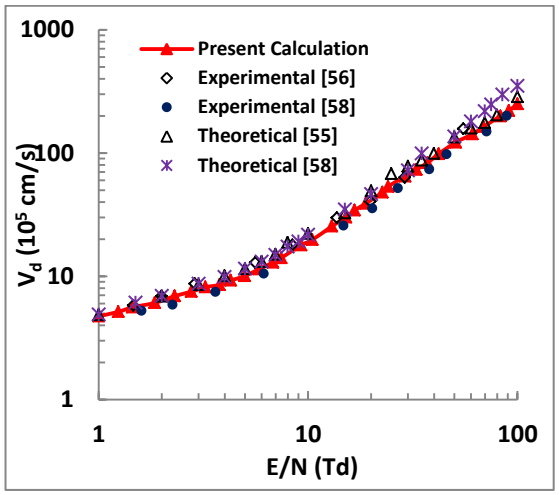

Figure 6: Electron drift velocity in pure helium

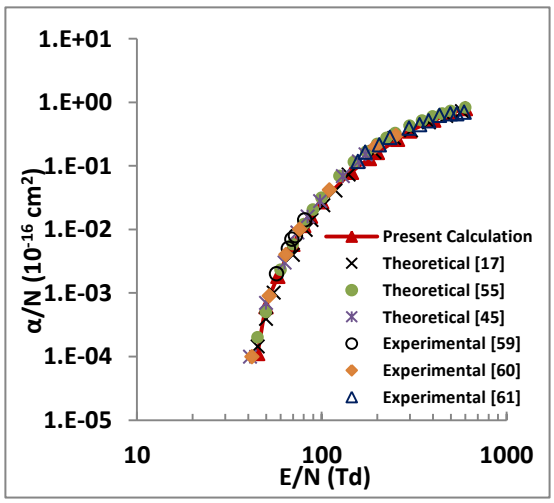

Figure 7: Density-reduced ionization coefficient in pure hydrogen.

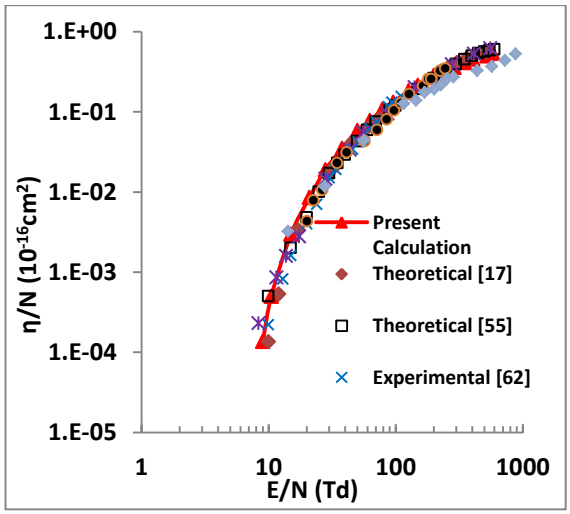

Figure 8: Density-reduced ionization coefficient in pure helium.

Flammability is a risk factor for hydrogen gas under atmospheric pressure and ambient temperature. To study dielectric strength of He-H_2 cryogenic gas mixture, before adding H_2 into He one should consider the flammable conditions that fail to propagate a flame in the mixtures. The values of the flammability limits of He-H_2 cryogenic gas mixtures are presented in Figure 9, and listed in Table 1 [29]. For gas mixtures with small concentration of H_2 over the range 1% to 9% safe flammability limits were observed.

Figure 10 shows the mean electron energy as a function of H_2 content in He-H_2 mixtures for a fixed value of E/N=10 Td, the mean energy is a summary of the electron energy distribution functions under specified conditions. Variation of the mean energy of the binary He-H_2 cryogenic gas mixtures as function of E/N are presented in Figure 11. The mean electron energy increased with increasing E/N, whereas, the tail of EEDF shifted to lower energy when the mole fraction of H_2 increased in the binary He-H_2 cryogenic gas mixtures. The mean electron energy of the mixtures has a trend to decrease with increasing H_2 content. The results showed a negative relation between the mean energy of the He-H_2 cryogenic gas mixtures and the mole fraction of H_2.

Table 1: Flammability limits of He-H_2 mixtures in air at T= 20^{o}C.

He in the fuel mixture % by vol.	Lean Limit	Rich Limit
0	3.9	74.1
20	4.8	75.3
40	6.6	76.3
50	8.0	77.6
60	10.0	77.5
80	21.9	78.5
90	53.0	79.0
91	61.1	79.0

The dependence of reduced electron mobility Nμ_e on reduced electric field E/N for different mole fraction of H_2 in cryogenic gas mixtures is represented in Figure 12. At low E/N values, the electron mobility decreased with increasing H_2 concentration at specified E/N values. While, at the interval E/N>10 Td, the behavior of electron mobility was reversed by increasing small mole fraction of H_2. As shown in Figure 4, at specified E/N=10 Td, the increase of H_2 concentration altered the EEDF by shifting it to lower energies, resulting in decreasing the mean electron energy, which effected the behavior of electron mobility, diffusion coefficient, ionization and attachment coefficient.

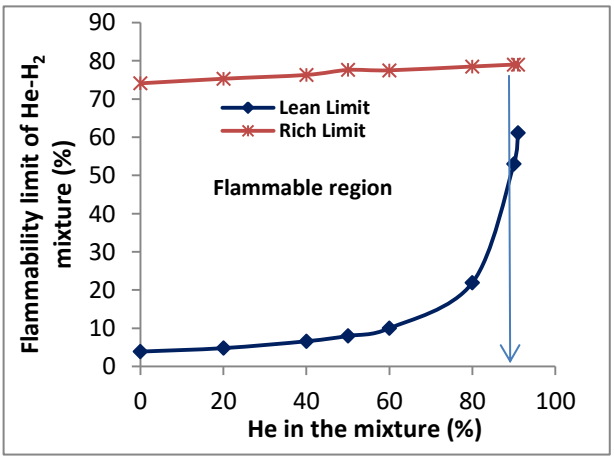

Figure 9: Flammability limits of He-H_2 mixtures in air as a function of He concentration in the fuel mixture, Experimental values from reference [29].

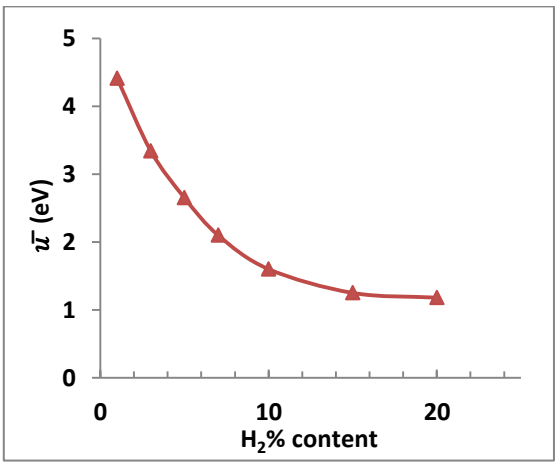

Figure 10: Mean electron energy in He-H_2 mixtures as a function of H_2% content at E/N= 10 Td.

The reduced-density transverse diffusion coefficient ND_T as a function of E/N for pure H_2, He and binary He-H_2 gas mixture is presented in Figure 13. The diffusion coefficient increased with increasing E/N, while negative correlation of the diffusion coefficient with the mole fraction of hydrogen at a fixed value of E/N in the binary He-H_2 cryogenic gas mixture was noticed, as shown in the figure. The diffusion coefficient of pure H_2 was lower than that of He. This difference refers to collisional electron cross-sections. Inelastic cross-sections (excitation, ionization and attachment cross –sections) require higher electron energy compared to elastic cross-sections ($(2m/M) \leq 10^{-4}$, where m is electron mass and M is molecule/atom mass), which effect the kinetic of electrons and EEDF reduce the electric field strength E/N as well as structure of a gas mixture effect the EEDF.

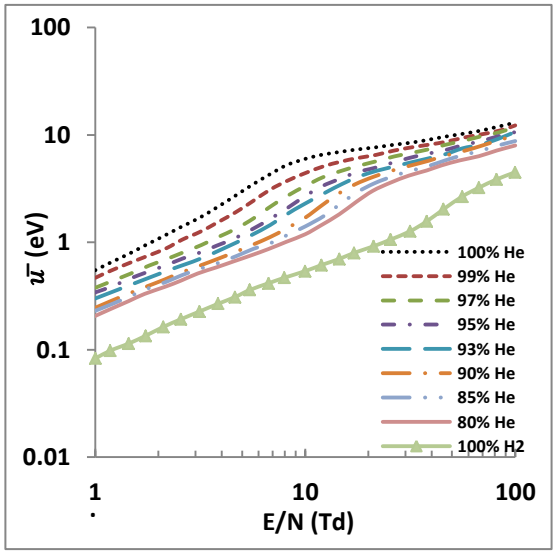

Figure 11: Mean electron energy in He-H_2 mixtures

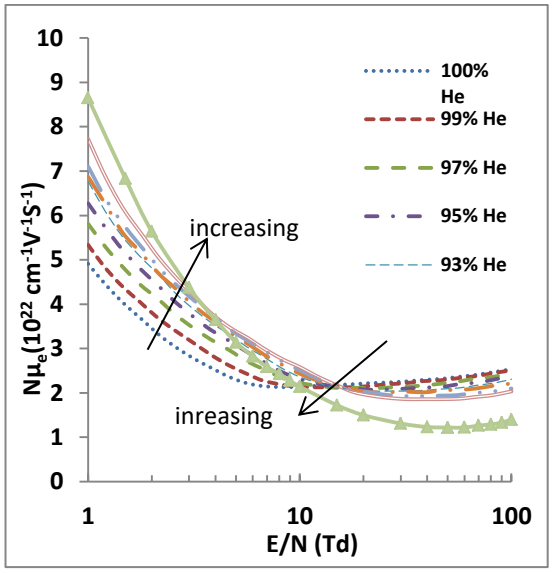

Figure 12: Density - normalized electron mobility in He-H_2 mixtures.

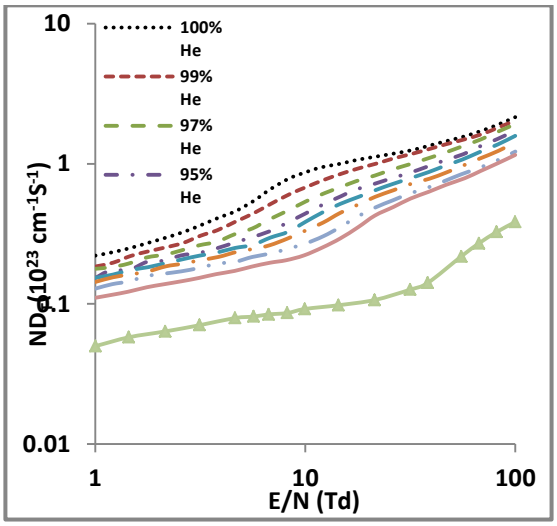

Figure 13: Density-normalized transverse diffusion coefficient in He-H_2 mixtures.

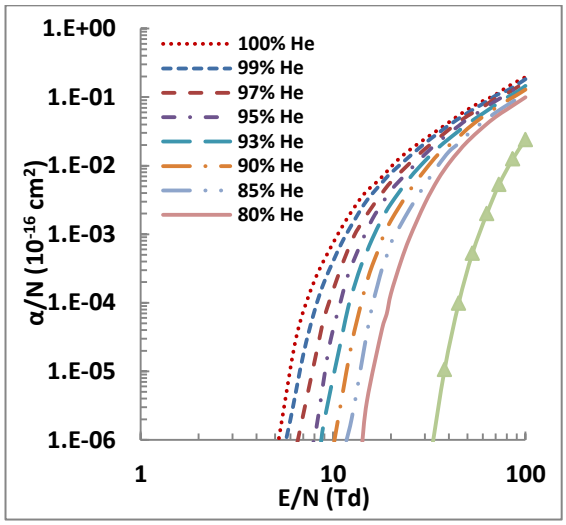

Figure 14: Density-reduced ionization coefficient in He-H_2 mixtures.

For all gases which display high dielectric field strength, the tail of EEDF shifts to the lower energy region. Figure 14 represents reduced density ionization coefficient α/N values of He-H_2 cryogenic gas mixture as a function of E/N, calculated values were based on EEDF by using two-term approximation solution of Boltzmann equation analysis (Eq. 11), using all types of collision cross-sections. Negative correlation of the reduced density ionization coefficient α/N with H_2 ratio in the gas mixture was noted. The calculated α/N values of He and H_2 together are shown in the same figure. In comparison, the α/N in H_2 was lower than that of He, over the same entire range. There are seven curves between He and H_2 with different ratio of H_2, i.e., 1%, 3%, 5%, 7%, 10%, 15%, and 20%. As shown in Figure 14, increasing the ratio of H_2 in the mixture led to the decrease of the ionization coefficient of the mixture. It is well known that the growth of the inelastic collisions depends on the electron energy and the hydrogen ratio in the mixture, for example the threshold energy of ionization potential of 15.427 eV, occurring at high electron energy, tends to reduce the number of fast electrons; decreasing mean electron energy results in shifting the tail of EEDF to the lower energy region, lowering the Townsend ionization coefficient as the mole fraction of hydrogen gas increased in the binary He-H_2 cryogenic gas mixture.

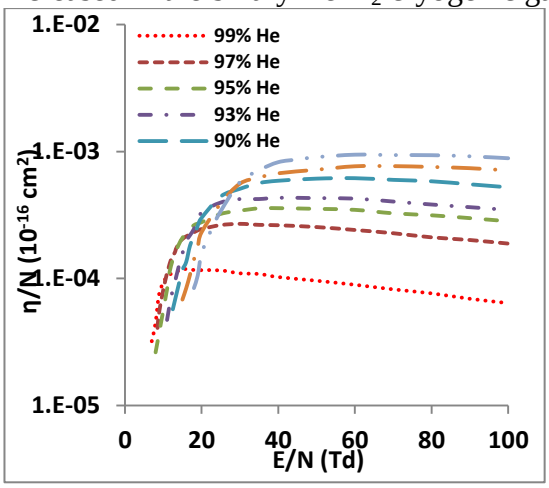

Figure 15: Density-reduced attachment coefficient in He-H2 mixtures.

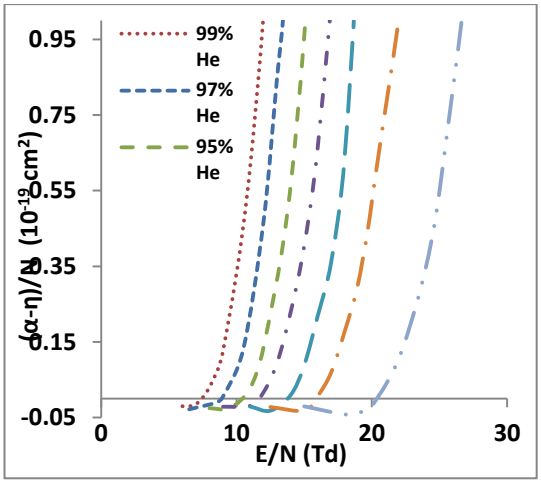

Figure 16: Density-reduced effective ionization coefficient in He-H2 mixtures.

The reduced density attachment coefficient η/N in He-H_2 mixture is shown as a function of E/N for different ratio H_2 in Figure 15. The value of η/N increased to a maximum value then started to decrease with increasing E/N. The behavior was observed for all values of H_2 mole fraction in binary He-H_2 cryogenic gas mixtures, the maximum value changed between 15 Td to 40 Td, due to diffusion loss in the mixture; when He is used as the buffer gas that has zero attachment cross-section, means that electrons cannot attach to helium atoms to form negative ions. Then the energy gains and losses are dominated by helium momentum transfer cross-sections. On the other hand, a positive correlation of η/N with the amount of hydrogen in the binary gas mixture was noted in the figure (direction of the arrow). However, the large collision ionization cross-section of helium and the small collision ionization cross-section of hydrogen, and different excitation collision cross-section of hydrogen contribute to create reduced density attachment coefficient η/N by shifting the tail of electron energy distribution function (EEDF) to lower energy region, it is the condition that attachment collision happen at low electron energy. Further decrease of α/N with the ratio of H_2 in the binary mixture, led to increase of η/N

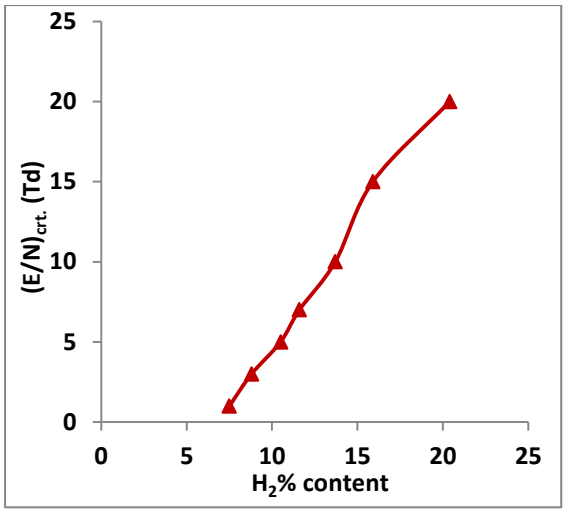

Figure 17: Density-reduced critical electrical field as a function of H_2% content in He-H_2 mixtures at T=77 K and P=2 MPa.

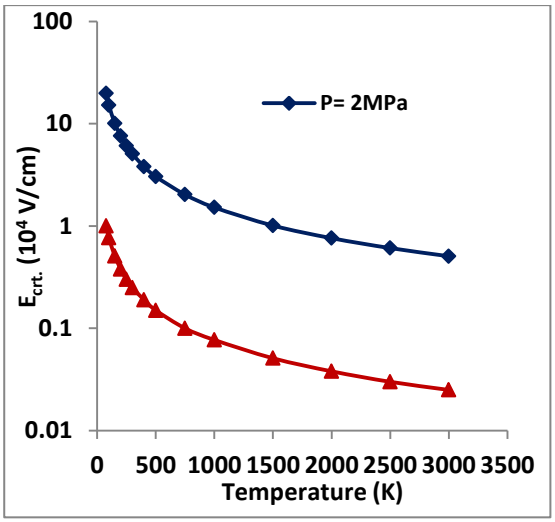

Figure 18: Critical electrical field as a function of pressure and temperatures for 95%He-5%H_2.

Based on the values of density-reduced ionization coefficient α/N and density-reduced attachment coefficient η/N, the density-reduced effective ionization coefficient (α-η)/N can be obtained, at which α/N and η/N are exactly balanced, (α-η)/N=0. This method was used by Itoh et al. [15]. From the curves of (α-η)/N as function of E/N, the density-reduced critical electric field $(E/N)_{crt}$ and critical breakdown electric field E_{crt} were defined as the E/N values at which (α-η)/N=0.

Figure 16 illustrates the density-reduced effective ionization coefficient (α-η)/N as a function of E/N in He-H_2 cryogenic gas mixtures at the ratios 99/1, 97/3, 95/5, 93/7, 90/10,85/15 and 80/20. With increasing H_2 mole fraction, the value of $(E/N)_{crt}$ increased strongly. Based on the data illustrated in Figure 16, it be noted that the value of $(E/N)_{crt}$ increased from 7.5 Td to 20.4 Td, as the mole fraction increased from 1% to 80%. Thus, it is clear that the increase of H_2 mole fraction in the mixture had significantly increased the probability of dielectric breakdown occurring in the binary He-H_2 cryogenic gas mixture at a fixed gas pressure 2MPa and temperature 77 K. The vibrational kinetics resulted in higher critical breakdown electric field, so the net electron production by ionization processes was low at high E/N, resulting in higher critical breakdown electric field.

The density-reduced critical electric field strength $(E/N)_{crt}$ for the He-H_2 cryogenic gas mixtures as function of H_2 content at pressure 2 MPa and temperature 77 K are presented in Figure 17 and listed in Table- 2. It is shown that as H_2 content increases, the reduced critical electric field $(E/N)_{crt}$ increases. Note that the critical breakdown electric field E_{crt} for pure helium is not listed in the table, because for helium η/N=0. In addition, the value of critical breakdown electric field E_{crt} for 95/5 He-H_2 mixture equal to 1.976 x 10^5 V/cm is in good agreement within the range of experimental breakdown voltage values of Graber et al. [8]. While, the real value of breakdown voltage of a mixture include secondary electron emission coefficient γ, according to relation $\gamma \exp(\alpha d) = 1 + \gamma^{-1}$ known as the Townsend breakdown criterion [30]; this value was not taken into account by the theoretical study using two-term solution of Boltzmann equation analysis. Therefore, the present value of critical breakdown electric field E_{crt} is in good agreement with the experimental values. E_{crt} shows the dielectric strength, obtained when $(E/N)_{crt}$ is multiplied by number density N. Note that the number

density N was calculated using the ideal gas law N= P/K_BT, where, P is the absolute pressure of a gas and T is absolute temperature, and K_B is Boltzmann constant =1.38 x 10^{-23} J/K.

Table 2: Critical electric field strength and electric field strength at temperature 77 K and pressure 2 MPa for different He-H_2 mixtures.

He-H_2 mixture (mol%)	N (cm^{-3}) 10^{21}	$(E/N)_{crt.}$ 10^{-17} Vcm^2	$E_{crt.}$ (V/cm) 10^5
99/1	1.882	7.5	1.411
97/3	1.882	8.8	1.656
95/5	1.882	10.5	1.976
93/7	1.882	11.6	2.183
90/10	1.882	13.7	2.578
85/15	1.882	15.9	2.992
80/20	1.882	20.4	3.839

In addition, the dielectric strength value of 95/5 He-H_2 at two different pressures as a function of temperature is shown in Figure 18. The dielectric strength decreased by increasing temperature because the dissociation processes increased with increasing temperature. Otherwise, the dielectric strength at pressure 2.0 MPa has a higher value compared to that at 1.01 x 10^5 KPa pressure at the same temperatures.

5. Conclusion

In this research the EEDF and electron swarm parameters, namely, (electron drift velocity, mean electron energy, electron mobility diffusion coefficient, ionization and attachment coefficient, density-reduced effective ionization coefficient, reduced critical electric field and critical electric field) in binary of H_2 gas with buffer He gas was calculated and analyzed using two-term solution of Boltzmann equation method over the range E/N varying from 1 to 100 Td at temperature 77 K and pressure 2 MPa. The change in the number of electron density (i.e. electron ionization and attachment) was taken into account to calculate EEDF, also the set of different cross sections play an important parameter for calculation the electron swarm parameters. The validity of the two-term approximation of Boltzmann equation in pure He and H_2 was confirmed over the entire range of E/N values. It was necessary to increase the momentum transfer cross-section slightly in order to obtain a good agreement between the present and previous theoretical and experimental results. The calculated electron swarm parameters (v_d, α/N and η/N) in pure He and H_2 were in good agreement with the available experimental and theoretical results. In the case of binary He-H_2 cryogenic gas mixture, the tail of EEDF shifted to lower energy region as the ratio of H_2 content in mixture was increased, α/N, (α-η)/N decreased, while, η/N, $(E/N)_{crt}$ and E_{crt} increased. The present result of critical field strength $E_{crt.}$= 9.8 x 10^4 V/cm is within the range of previous experimental value. It was found that higher E_{crt} is obtained at higher pressure 2.0 MPa and lower temperature 77 K. Furthermore, the mean electron energies at constant E/N value, decreased with increasing H_2 in the mixture.

References

[1] C. Park, L. Graber and S. Pamidi, "The dielectric properties of gaseous cryogen mixtures of He, H2, Ne, and N2 in a temperature range of 50–80 K at pressures up to 2.0 MPa," *Journal of Applied Physics*, vol. 121, no. 8, p. 083304, 2017.

[2] S. Pamidi, C. H. Kim and L. Graber, "*High-temperature superconducting (HTS) power cables cooled by helium gas," in In Superconductors in the Power Grid, The Florida State University, Tallahassee, FL, USA, Woodhead Publishing*, 2015, pp. 225-260.

[3] L. Graber, C. H. Kim and S. V. Pamidi, "Dielectric design validation of a helium gas cooled superconducting DC power cable," in *IEEE Electrical Insulation Conference* (EIC), 8-11 June, pp. 157-161, Philadelphia, PA, USA, 2014.

[4] M. J. Pinheiro and J. Loureiro, "Effective ionization coefficients and electron drift velocities in gas mixtures of SF6 with He, Xe, CO2 and N2 from Boltzmann analysis," *Journal of Physics D*: Applied Physics, vol. 35, no. 23, pp. 3077-3084, 2002.

[5] H. Zhao, X. Li, S. Jia and . A. B. Murphy, "Prediction of the critical reduced electric field strength for carbon dioxide and its mixtures with 50% O2 and 50% H2 from Boltzmann analysis for gas temperatures up to 3500 K at atmospheric pressure," *Journal of Physics D: Applied Physics*, vol. 47, no. 32, p. 325203 (10 pp), 2014.

[6] S. S. Tezcan, M. S. Dincer, . S. Bektas and . H. R. Hiziroglu, "Boltzmann analysis of electron swarm parameters in binary CF4+ Ar mixtures," *IEEE Transactions on Dielectrics and Electrical Insulation*, vol. 20, no. 1, pp. 98-103, 2013.

[7] Y. Deng, . B. Li and . D. Xiao, "Analysis of the insulation characteristics of C3F8 gas mixtures with N2 and CO2 using Boltzmann equation method," *IEEE Transactions on Dielectrics and Electrical Insulation*, vol. 22, no. 6, pp. 3253-3259, 2015.

[8] L. Graber, W. J. Kim, P. Cheetham, C. H. Kim, H. Rodrigo and S. V. Pamidi, "Dielectric properties of cryogenic gas mixtures containing helium, neon, and hydrogen," in In *IOP Conference Series: Materials Science and Engineering* (Vol. 102, No. 1, p. 012018), Tucson, AZ, USA, 2015.

[9] P. Cheetham, C. Park, . C. H. Kim, L. Graber and S. V. Pamidi, "Dielectric properties of cryogenic gas mixtures for superconducting power applications," in *In IOP Conference Series: Materials Science and Engineering* (Vol. 278, No. 1, p. 012040), Madison, Wisconsin, USA, 2017.

[10] C. Park, . L. Graber, . P. Cheetham, A. Al-Taie, S. elikapalli and S. Pamidi, "Versatile Paschen's model for the dielectric strength estimation of binary and ternary gas mixtures," *IEEE Transactions on Dielectrics and Electrical Insulation*, vol. 26, no. 5, pp. 1569-1576, 2019.

[11] K. Smith and R. M. Thomson, Computer Modeling of Gas Lasers, *New York: Plenum Press*, 1978.

[12] L. S. Frost and A. V. Phelps, "Rotational excitation and momentum transfer cross sections for electrons in H2 and N2 from transport coefficients," *Physical Review*, vol. 127, no. 5, pp. 1621-1633, 1962.

[13] Y. Nakamura and . J. Lucas, "Electron drift velocity and momentum cross-section in mercury, sodium and thallium vapours. II. Theoretical," *Journal of Physics D: Applied Physics*, vol. 11, no. 3, pp. 337-345, 1978.

[14] L. Laska, . K. Mašek, J. Krasa and V. Peřina, "Dielectric properties of SF6 mixtures containing oxygen and other gases," *Czechoslovak Journal of Physics B*, vol. 34, no. 10, pp. 1038-1047, 1984.

[15] H. Itoh, M. Shimozuma and H. Tagashira, "Boltzmann equation analysis of the electron swarm development in SF6 and nitrogen mixtures," *Journal of Physics D: Applied Physics*, vol. 13, no. 7, pp. 1201-1209, 1980.

[16] L. J. Kieffer, "*A compilation of electron collision cross section data for modeling gas discharge lasers," JILA information center report 13, University of Colorado, Boulder, Colorado, US*, 1973.

[17] S. D. Rockwood and A. E. Greene, "Numerical solutions of the Boltzmann transport equation," *Computer Physics Communications*, vol. 19, no. 3, pp. 377-393, 1980.

[18] A. G. Engelhardt and . A. V. Phelps, "Elastic and inelastic collision cross sections in hydrogen and deuterium from transport coefficients," *Physical Review*, vol. 131, no. 5, pp. 2115-2128, 1963.

[19] W. Roznerski and . K. Leja, "Electron drift velocity in hydrogen, nitrogen, oxygen, carbon monoxide, carbon dioxide and air at moderate E/N," *Journal of Physics D: Applied Physics*, vol. 17, no. 2, pp. 279-285, 1984.

[20] P. Thi Lan and B. H. Jeon, "Determination of Electron Collision of Cross-Sections for the H2 Molecule for Plasma Discharge Simulation," *Journal of the Physical Society of Japan*, vol. 81, no. 10, p. 104501(7pp), 2012.

[21] G. G. Raju, Gaseous electronics: tables, atoms, and molecules, New York: CRC Press, 2018.

[22] H. N. Kucukarpaci, H. T. Saelee and J. Lucas, "*Electron swarm parameters in helium and neon," Journal of Physics D: Applied Physics*, vol. 14, no. 1, pp. 9-25, 1981.
[23] D. A. Tuan, "Analysis of electron transport coefficients in binary mixtures of TEOS gas with Kr, Xe, He and Ne gases for using in plasma assisted thin-film deposition," *Journal of Electrical Engineering and Technology*, vol. 11, no. 2, pp. 455-462, 2016.
[24] Michael A. Lieberman and Alan J. Lichtenberg, *Principles of Plasma Discharges and Materials Processing, Canada: John Wiley & Sons, Inc*, 2005.
[25] D. J. Rose, "Townsend ionization coefficient for hydrogen and deuterium," *Physical Review*, vol. 104, no. 2, pp. 273-277, 1956.
[26] M. A. Shallal and J. A. Harrison, "Pre-breakdown currents in hydrogen in uniform and non-uniform fields," *Journal of Physics D: Applied Physics*, vol. 4, no. 10, pp. 1550-1559, 1971.
[27] L. M. Chanin and G. D. Rork, "Experimental determinations of the first Townsend ionization coefficient in helium," *Physical Review*, vol. 133A, no. 4, pp. 1005-1009, 1964.
[28] C. S. Lakshminarasimha, J. Lucas and R. A. Snelson, "Time-of-flight electron-swarm studies of ionisation and attachment in gases," *Proceedings of the Institution of Electrical Engineers*, vol. 122, no. 10, pp. 1162-1165, 1975.
[29] M. Terpstra, "Flammability limits of hydrogen-diluent mixtures in air," Master's thesis, Graduate Studies, University of Calgary, p. 28, 2012.
[30] A. Küchler, *High Voltage Engineering: Fundamentals-Technology-Applications, GmbH Germany: Springer-Verlag*, 2018.